LA-UR-06-2087



*Title:* UNCERTAINTY, MODEL ERROR, AND IMPROVING THE ACCURACY OF RESIDUAL STRESS INVERSE SOLUTIONS

*Author(s):* Michael B. Prime (ESA-WR)
Pierluigi Pagliaro (ESA-WR)

*Submitted to:* Proceedings of the 2006 SEM Annual Conference and Exposition on Experimental and Applied Mechanics, paper number 176 (CD-ROM proceedings)

# Uncertainty, Model Error, and Improving the Accuracy of Residual Stress Inverse Solutions

Michael B. Prime, Technical Staff Member (prime@lanl.gov)
Los Alamos National Laboratory, Los Alamos, NM 87545

Pierluigi Pagliaro, Ph.D. student (pagliaro@dima.unipa.it)
Dipartimento di Meccanica, Universitá degli Studi di Palermo, Palermo, Italy 90128
Visiting Researcher, Los Alamos National Laboratory, Los Alamos, NM 87545

## ABSTRACT

A new approach for estimating total uncertainty in residual stress inverse solutions is used to improve the accuracy of the solutions by optimizing experimental and analytical methods. Inverse solutions provide a special challenge for uncertainty analysis. The traditional uncertainty analysis, based on propagating uncertainties in the measured quantities through the equations, can give grossly underestimated uncertainties. Often a more significant error source is "model error," the error caused by the actual stress distribution not matching the assumptions, or model, used to solve the inverse problem. A new approach to estimate both traditional uncertainty and model error in series expanded solutions to a Volterra equation is reviewed. Such inverse problem solutions are used for residual stress measurements using the slitting method (crack compliance), hole drilling, layer removal, and some eigenstrain methods. In this paper, the new approach to estimate uncertainty is used to improve the accuracy of slitting method inverse solutions both in the analytical approach and by optimizing experimental parameters such as the number of data points taken.

## Introduction

Residual stress measurements often rely on the solution of elastic inverse problems to determine residual stresses from measured deformation data. Inverse solutions can have a drastic effect on the uncertainties in the measured data, such as magnifying the data errors into larger stress errors. A new uncertainty analysis has for the first time allowed an accurate estimate of uncertainties for residual stress inverse solutions [1]. This uncertainty analysis particularly applies to series expanded inverse solutions. The analysis allows not only accurate uncertainty estimates but also allows the objective selection of the optimal order of the series expansion. The series expansion approach to the inverse solution is used for measurement techniques such as hole drilling, layer removal, sectioning, Sachs' boring out, and many other methods. In this paper, we apply the method to the incremental slitting method, previously called the crack compliance method.

This paper focuses on optimizing the number slit depths, which is the number of data points, for the incremental slitting method. Slitting is being developed as an ASTM standard in Task Group E28.13.02. The number of slits depths must be specified for the standard, and an rational requirement is desired. More slit depths require more effort but help reduce the effect of experimental noise. In order to isolate error sources in this study, a numerical simulation is used for the study of experimental errors.

## The Slitting Method & Inverse Solution

In the slitting method, Figure 1, a narrow slit is incrementally cut into a part containing residual stresses. Stresses are relaxed and the part deforms, which is assumed to occur elastically. At an appropriate location strains are measured at discrete slit depths, *a*,

$$\varepsilon(a_i) = \varepsilon_i \tag{1}$$

where there are *m* slit depths *i* = 1,*m*. This is the main parameter that will be varied in this study. We will also refer to this as "number of cuts."

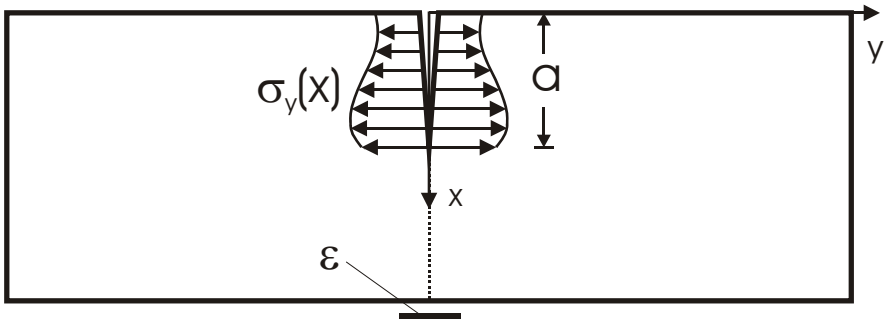


Figure 1. The incremental slitting method for measuring residual stress.

Assuming that the stresses do not vary in the z-direction, the strain measured at an arbitrary cut depth is related to the residual stresses that originally existed on the plane of the cut by a Volterra equation of the first kind

$$\varepsilon(a) = \int_0^a c(a,x)\sigma_y(x)dx\,, \tag{2}$$

where $c$ is a function of the geometry and the material elastic constants. Since a closed-form inverse solution for $\sigma_y(x)$ is not available, it is assumed that the stress can be approximated as a series expansion in analytic basis functions

$$\sigma_y(x_i) = \sigma_i = \sum_{j=1}^{n} A_j L_{j+1}(x_i) = [L]\{A\}\,. \tag{3}$$

Legendre polynomials are used as the basis functions for through-thickness stresses because omitting the uniform and linear polynomials enforces equilibrium. Thus the expansion in Eq. 3 starts with the 2nd order Legendre polynomial. The second equality introduces matrix notation for convenience; [$L$] has rows corresponding to spatial positions $x_i$ and columns corresponding to terms $j$ in the series expansion. The solution for $\sigma$ now requires choosing an expansion order $n$ and determining the basis function amplitudes $A_j$. The solution strategy requires determining the strain release $C_j(a_i)$ that would occur at $a = a_i$ if $\sigma_y(x)$ were exactly given by $L_{j+1}(x)$. Using elastic superposition, the strain that would be measured for the $\sigma_y(x)$ from Eq. 3 is then given by

$$\varepsilon_f(a_i) = \varepsilon_{f,i} = \sum_{j=1}^{n} A_j C_j(a_i) = [C]\{A\} \tag{4}$$

where the subscript $f$ refers to these calculated strains being determined by a least squares fit minimizing the difference between the measured strains, $\varepsilon$, and calculated strains:

$$\{A\} = \left[ \left( [C]^T [C] \right)^{-1} [C]^T \right] \{\varepsilon\} = [B]\{\varepsilon\}\,. \tag{5}$$

## Uncertainty Analysis

**Propagated Uncertainty**. The salient equations from the previously derived uncertainty analysis [1] are repeated here. The uncertainty in the calculated stress at each depth is determined from a first order expansion of the propagated uncertainty in the fit coefficients:

$$s_i^2 = u_{A_1}^2 \left( \frac{\partial \sigma_i}{\partial A_1} \right)^2 + u_{A_2}^2 \left( \frac{\partial \sigma_i}{\partial A_2} \right)^2 + \ldots + 2u_{A_1A_2}^2 \left( \frac{\partial \sigma_i}{\partial A_1} \right) \left( \frac{\partial \sigma_i}{\partial A_2} \right) + \ldots \tag{6}$$

where generally $u_h$ is used for uncertainty in a parameter $h$, but $s$ instead is used for uncertainty in stress in order to simplify notation later on. For the major source of experimental uncertainty, the measured strains, the matrix of the covariances of the $A_i$ is calculated considering the uncertainty in the measured strains

$$u_{A_k A_l}^2 = \sum_{i=1}^{m} \left[ u_{\varepsilon,i}^2 \frac{\partial A_k}{\partial \varepsilon_i} \frac{\partial A_l}{\partial \varepsilon_i} \right]. \tag{7}$$

where $u_{\varepsilon,i}$ is the uncertainty in the strain measured when $a = a_i$. Using Eqs. 3 and 5 in Eqs. 6 and 7, the propagated uncertainty in the stress is

$$\left\{s_{\varepsilon,i}^2\right\} = \mathrm{diag}\left([L][B]\left[\mathrm{DIAG}\left\{u_\varepsilon^2\right\}\right][B]^T[L]^T\right) \tag{8}$$

where *DIAG* indicates a diagonal matrix whose diagonal elements are the elements of the vector and *diag* indicates forming a column vector from the diagonal elements of a matrix. The additional subscript $\varepsilon$ on $s$ indicates that the source of this stress uncertainty is the uncertainty in the measured strains. To avoid confusion with the uncertainty in the strains themselves, $u_{\varepsilon,i}$, this uncertainty in stress will be referred as "measurement" uncertainty.

The inherent uncertainty of the measurement equipment should be the primary estimate of uncertainty in the measured strains. However, this parameter can be quite difficult to accurately estimate. If a large enough number of cut depths is used, the misfit between the data itself and a smooth curve can provide a supplemental estimate of the strain uncertainty. An estimate of the standard deviation of the strain misfit, unbiased by the number of degrees of freedom in the series expansion, is given by

$$\overline{u}_\varepsilon = \sqrt{\frac{1}{m-n}\sum_{i=1}^{m}\left(\varepsilon_i - \varepsilon_{f,i}\right)^2} \tag{9}$$

where the overbar indicates a root-mean-square (rms) average over all measured strains. To be consistent with this average, the uncertainty of an individual value can be taken as

$$u_{\varepsilon,i} = \sqrt{\frac{m}{m-n}}\left|\varepsilon_i - \varepsilon_{f,i}\right|. \tag{10}$$

**Model Error/Uncertainty**. In the general case when actual stresses cannot be perfectly fit by the chosen series expansion, a conventional analysis of all the propagated uncertainties fails to adequately estimate total uncertainty. The propagated uncertainty analysis implicitly assumes that the "model," the series expansion, can match the actual stress. When it cannot match, the uncertainty is underestimated. To estimate the model error, stresses for different values of $n$ are calculated. At each depth where stress is calculated, $x_i$, we take a standard deviation of the stresses calculated for different order expansions

$$s_{model,i}^2(n) \approx \frac{1}{N-1}\sum_{k=n-1}^{n+1}\left(\sigma_i(n=k) - \overline{\sigma}_i\right)^2 \tag{11}$$

where the average stress at $x = a_i$, $\overline{\sigma}_i$, is averaged over the expansion orders from $n$-1≤ $k$ ≤ $n$+1 but not averaged over other $x$ positions. $N$ is the number of stress solutions in the sum,3. The calculation is repeated at each $x$ where stress is evaluated.

**Total Uncertainty.** The total uncertainty is obtained by pointwise combining the individual uncertainties in quadrature since they are assumed to be independent

$$s_{total,i} = \sqrt{s_{\varepsilon,i}^2 + s_{model,i}^2} \tag{12}$$

from which an average uncertainty $\overline{s}_{total}$ can be calculated using an rms average over the cut depths.

## Numerical Simulations

A numerical study was used to determine the effect of an important experimental parameter: $m$, the number of slit depths. In the presence of random experimental noise, it was postulated that increasing the number of experimental points would result in lower errors. It was desired to estimate an optimal number of cut depths by determining when further increases in the number of cut depths began to have diminishing improvements in errors in the final stresses. It was also postulated that to some extent, increasing the number of cut depths would increase the spatial resolution of the results. Increased resolution would be reflected in better results with higher order expansions. Finally, it was desired to check the accuracy of the uncertainty analysis and the ability of the analysis to select the truly optimal expansion order.

A beam with thickness of $t$ = 1 was simulated and the beam was 10$t$ long. A zero-width slit was considered at the exact mid-length of the beam. The slit was extended in increments of d$a$ = 0.02$t$ to a final depth of $a$ = 0.96$t$ giving $m$ = 48 depths. The strains were calculated for a strain gage with length 0.01$t$ centered directly opposite the slit. Since 2D solutions under applied loads and free of body forces are independent of elastic constants, the material behavior was conveniently taken as elastic with an elastic modulus of 1 and Poisson's ratio of zero.

**Test Case Stresses**. A realistic residual stress profile is used for the numerical simulation. It is profile that might be produced by introducing compressive stresses on one surface of a beam to a depth about 25% of the thickness. Such stresses might be induced by shot peening, laser peening, case hardening, or some other surface treatment process. The profile came from the Gaussian function so that it could not be fit exactly by polynomials and could therefore be expected to have significant model error. A linear term was added to the Gaussian function to establish force and moment equilibrium, and the profile was normalized to give a peak compressive stress of negative one. The Gaussian distribution is given by

$$\sigma(x) = 2.28735\left(0.609825 - 0.857365x - e^{-\left(\frac{x-0.05}{0.15}\right)^2}\right). \qquad (13)$$

And is shown in Figure 2.

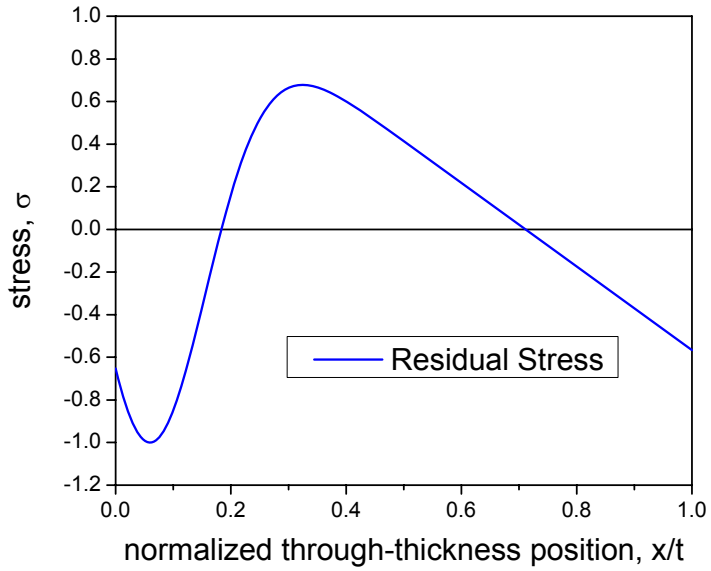


Figure 2. Residual stress distribution used for numerical simulations.

By using the same finite element model to simulate the slitting experiment and to calculate the calibration coefficients $C_j(a_i)$, no additional error sources enter the simulation. Using symmetry about the cut plane, half of the beam was modeled using 8-noded, quadratic shape function quadrilateral elements. On the cut plane, the mesh had 200 elements through the thickness of the beam, transitioning to a coarser mesh farther away. Incremental slit extension was simulated by removing the appropriate symmetry nodal displacement constraints on the slit plane in sequential analysis steps. To calculate the calibration coefficients, the element edges defining the exposed face of the slit were loaded with a non-uniform pressure distribution sequentially corresponding to $L_2(x)$ through $L_{16}(x)$. The remaining surfaces are taken as traction free. To calculate the strains for the stress profile in Figure 2, the analysis was repeated for pressure distributions corresponding to Eq. 13. Finally, strain for the gage centered on the symmetry plane was calculated by computing the relative displacement of the nodes corresponding to the center and end of the strain gage and dividing by initial length between the nodes. Figure 3 shows the simulated strains.

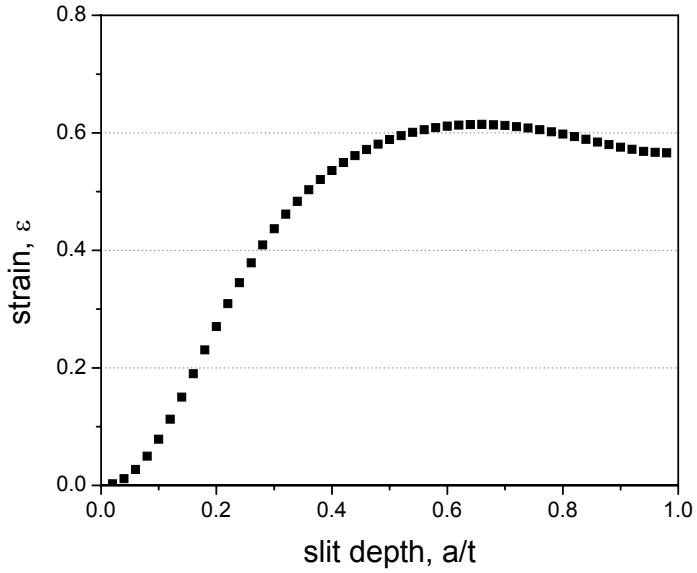


Figure 3. Simulated strains measured during slitting experiment.

**Evaluating the Number of Cuts**. Building on the previous work on uncertainty analysis [1], a numerical procedure was used to simulate the effect of changing the experimental number of cuts, *m*. The following outline shows the basic procedure, which is then explained in greater detail

1. Vary the number of cuts, *m.*
    1.1. Add simulated noise to the strain data.
        1.1.1. Calculate stress results for all the possible expansion orders.
        1.1.2. Calculate errors and uncertainty estimates.
    1.2. Repeat 1.1 with different set of random noise in order to get statistical estimate
    1.3. Calculate average errors from 1.1.2 over all sets of random noise from 1.2.
2. Repeat 1 for different number of cuts.

**Vary the number of cuts**. The minimum number of cut depths considered was two so that an over-determined least squares fit was possible using a 1 term series expansion. The maximum number of cut depths considered was 100, which exceeds the maximum number that has ever been reported [2]. To simulate changing the number of slit depths, the calibration coefficients $C_j(a_i)$ and the simulated measured strains (Figure 3) were spline interpolated to different numbers of slit depths. The slit depths were always equally spaced to a final depth of 0.96.

**Add simulated noise to the strain data**. Measurements in the presence of experimental errros were tested by simulating noise in the measured strain data. A realistic range of strain noise magnitudes were considered. In practice, the largest strain noise or errors occur when the strain magnitudes are the lowest. About the lowest strain magnitudes reported for slitting measurements were strains that peaked at about 40 $\mu\varepsilon$ [3]. In such a case, strain errors of a few microstrain would make the error magnitudes about 10% of the peak magnitudes. On the other end of the scale, peak magnitudes exceeding 1000 $\mu\varepsilon$ are often measured. One might hope to keep the strain errors below 1 $\mu\varepsilon$, keeping errors below 0.1% of peak magnitudes. Errors at 0.5% of peak magnitude are probably more realistic. In any case, we also report results for perfect data with no errors for informational purposes.

The simulated measured strains from Figure 3 were randomized by adding an uncertainty vector

$$\{\varepsilon_r\} = \{\varepsilon\} + \{u_\varepsilon\}. \tag{14}$$

Each $u_{\varepsilon,i}$ was selected from zero-mean normal distribution using a random number generator. To examine different magnitudes of noise, the distribution was scaled to different standard deviations. Results varied significantly between different sets of random strain added to the strain data. Therefore, to establish the average trends, each test case was repeated with 500 sets of randomized noise added to the strain data, each from the

same underlying population of a given standard deviation and zero mean. The strain errors are reported as the standard deviation of $u_\varepsilon$ relative to the peak strain of 0.614 in Figure 3.

**Calculate stress results for all the possible expansion orders**. Each test case was examined over a large range of expansion orders, $n$ =1 to 15. The $A_j$ were calculated from Eq. 5, with $\{\varepsilon_i\}$ replacing $\{\varepsilon\}$ for the cases where noise in the strain data was simulated. The resulting stresses and fit strains were calculated using Eqs. 3 and 4. The stress uncertainty from random errors in the strain data were then evaluated using Eqs. 8 and 10. The model uncertainties were evaluated using Eq. 11. For the noise-added test cases, the same set of noisy strain data was used for all 15 expansion orders before a new set was generated.

**Calculate errors and uncertainty estimates**. The actual error $e$ is evaluated by comparing the calculated residual stress distribution with the known stresses of Eqs. 13. The pointwise error at each $x_i$ is just the difference between the calculated, $\sigma_{c,i}$, and known stresses, $\sigma_{k,i}$. A root-mean-square average value is calculated from the pointwise values:

$$\bar{e} = \sqrt{\frac{1}{m}\sum_{i=1}^{m}\left(\sigma_{c,i} - \sigma_{k,i}\right)^2} \qquad (15)$$

In order to provide a fair comparison, the stresses and errors are always evaluated at the original 48 slit depths, regardless of the number of slit depths being considered in a particular trial. Because the stress profiles were normalized to give a peak magnitude of one, all of the stress errors and uncertainties can be considered as normalized to the maximum stress magnitude in the residual stress profile. Similar depth-averaged values were calculated for the measurement, model, and total uncertainties. The depth-averaged errors and uncertainties do not include the values at $x$ = 0, which is considered an extrapolated value since the first data point is taken at the first cut depth.

Each depth-averaged error or uncertainty was then averaged over the 500 trials with different noise added to the data.

## Results and Discussion

**Typical results**. Before looking at the results for different numbers of slit depths, it is instructive to look at results for a fixed number of cut depths. Figure 4 shows the results for 35 cuts and strain error = 0.002 or about 0.33% of the peak strain from Figure 3. The results, averaged over 500 sets of random strain error added to the data, are fairly typical. The actual errors from Eq. 15 show a minimum at $n$ = 9, which is therefore the best achievable solution using a Legendre series expansion. The measurement uncertainty from Eq. 8 tends to match the actual errors for higher expansion orders. The model uncertainty from Eq. 11 tends to match the errors at lower expansion orders. Therefore, the total uncertainty from Eq. 12 tends to match the actual errors over the entire range, and shows a minimum at $n$ = 8, close to the minimum in actual error.

**Best Achievable Results.** First we examine the best achievable results, independent of our ability to accurately estimate uncertainty or to objectively select the best expansion order.

Figure 5 shows the minimum in actual error as a function of number of slit depths for different levels of noise added to the strain data. The general trends meet expectations. The minimum actual error generally decreases as the number of cuts increases, with eventual diminishing returns. The overall error levels increase as the strain errors increase. The inverse solution has resulted in amplified errors: the stress errors usually exceed the corresponding strain errors.

The results provide good guidance on the optimal number of experimental cuts, with 25 cuts appearing to be a minimum to achieve optimal results. Almost all of the curves in Figure 5 decrease quite steeply until there are at least 25 cuts. Depending on the level of noise added to the strain data, the curves continue to decrease significantly until 30 to 40 cuts. For the higher noise levels, significant improvements in stress errors are possible up to 50 cuts and beyond.

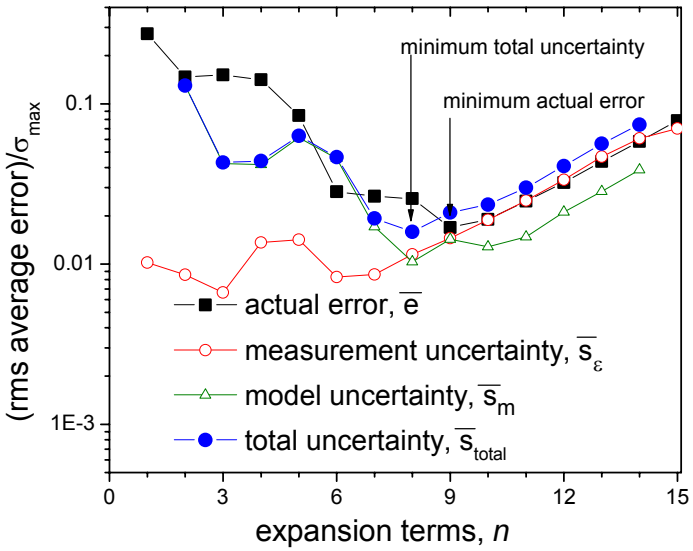


Figure 4. Results for 35 cut depths and strain noise = 0.33% of the peak strain magnitude. These results are averaged over 500 trials with different sets of random noise added to the strain data.

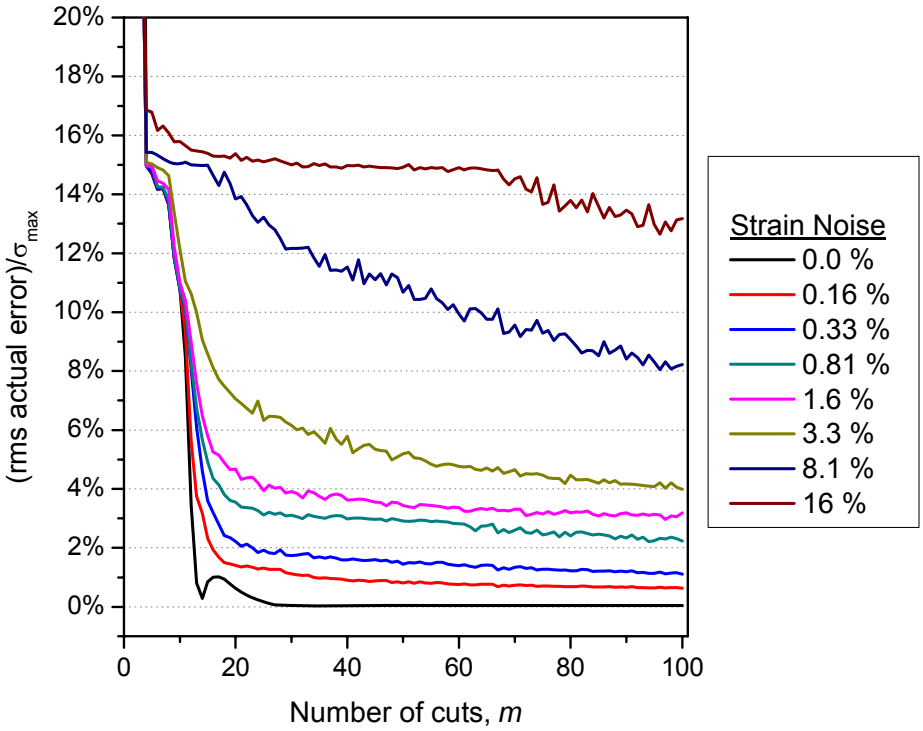


Figure 5. Best achievable errors as a function of number of cuts. The levels of noise in the strain data correspond to $u_\varepsilon$ in Eq. 14.

Figure 6 shows the expansion orders, *n* in Eq. 3, that correspond to the minima in total error plotted in Figure 5. Because it minimizes the actual errors, these expansion orders represent the optimal choice for expansion order. The expansion order also indicates spatial resolution since the higher order polynomials have shorter wavelengths. Again we see the expected trends. The optimal expansion order increases with the number of cuts, especially until there are at least 20 cuts. As the level of error in the strain data increases, the optimal expansion order decreases. Therefore, increasing noise levels decreases the spatial resolution of the results.

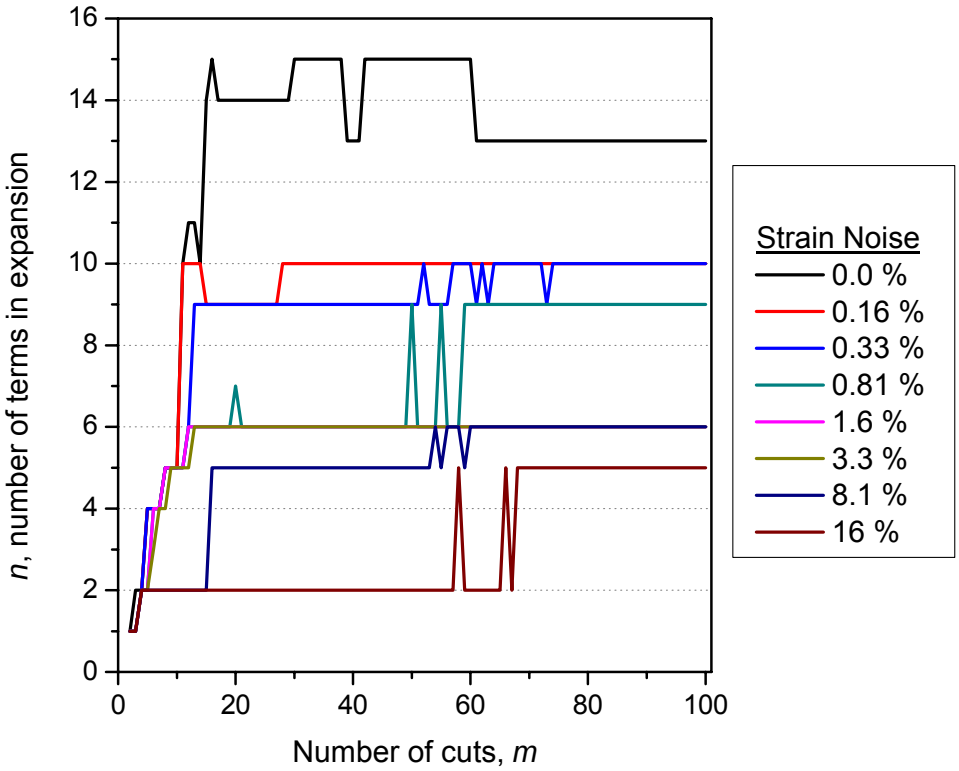


Figure 6. Expansion orders corresponding to minima in actual error.

**Performance of the uncertainty estimation procedure**. Since the actual errors cannot be known in a real measurement, it is desired to select the optimal expansion order and to estimate the uncertainties as accurately as possible. So far, the best method for making these estimates is to select the expansion order based on the minimum estimated total uncertainty and to use that uncertainty estimate [1]. The key aspect of the achieving a good result is the selection of the optimal expansion order.

Figure 7 shows the expansion order chosen objectively by the uncertainty analysis procedure. It is chosen on the basis of minimum total uncertainty. Comparing with Figure 6 shows that the overall trends are correct. The estimated optimal expansion order agrees with the actual optimal expansion order sometimes, and sometimes it does not. Considering the statistical nature of the problem, the occasional discrepancy is expected. The difficulty in estimating the optimal order comes mostly from the difficulty in estimating the model uncertainty, which is very difficult because of the nature of model error. In the particular stress profile studied here, the model error estimate gives poor results for $n$ = 3 and 4, as seen in Figure 4. As the strain errors increase, the optimal expansion order moves lower towards $n$ = 3 and 4, and this causes errors in the selection of optimal expansion order. The difficulty picking the optimal expansion order for higher noise is specific to the stress distribution studied here and not a general result.

Figure 8. Shows the total estimated uncertainty, which corresponds with the expansion order from Figure 7. The overall trends and magnitudes are similar to Figure 5. Realize that the analysis should match the actual errors for the expansion orders in Figure 7. If the selected expansion order matches the actual optimum from Figure 6, then the errors should match Figure 5. When the correct optimal expansion order is selected, the total estimated uncertainty tends to slightly overestimate the total actual error. The overestimation occurs because the model uncertainty overestimates the actual model error as the expansion order increases [1]. However, for fewer cut depths, the overestimation decreases and eventually the total error is underestimated.

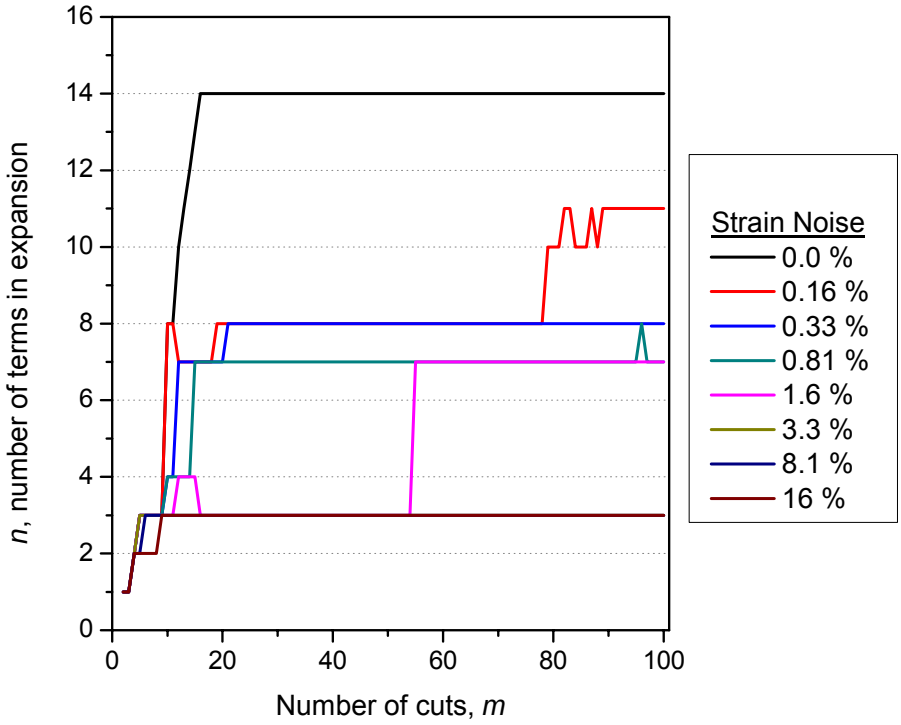


Figure 7. Expansion order for the minimum in total estimated uncertainty.

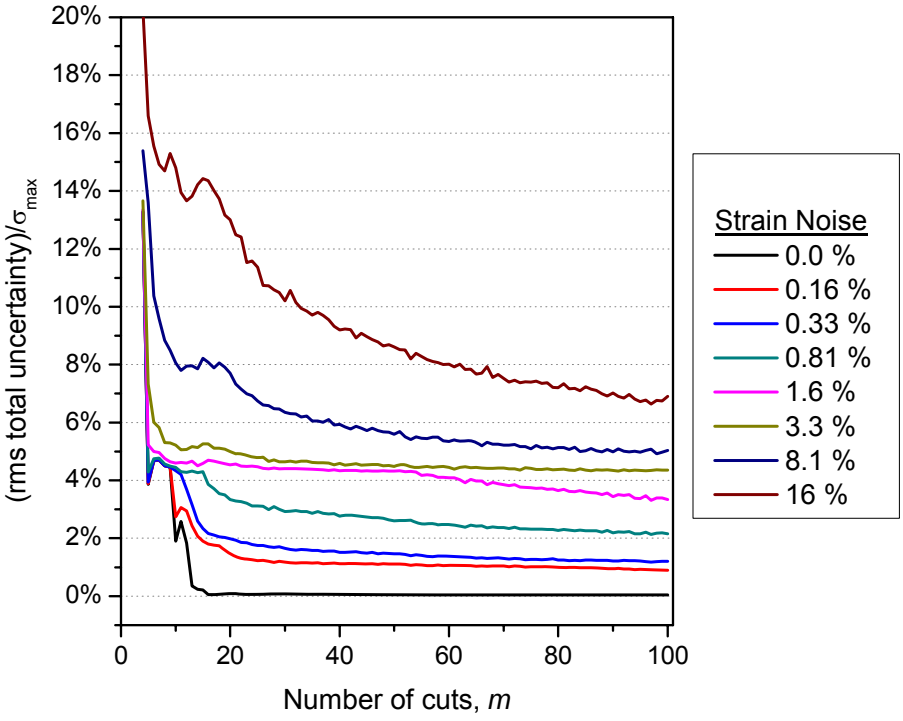


Figure 8. Estimated total uncertainty.

Figure 9. Shows the estimated measurement uncertainty, which is the total uncertainty with the model uncertainty removed. This is the result one would get if model error were ignored. As discovered previously [1], the measurement uncertainty provides a better estimate than the total uncertainty of the actual error for higher order fits and more statistically significant samples, which in this case means more cut depths. However, it

underestimates the actual error for fewer cut depths even more significantly than Figure 8, giving further evidence of the importance of estimating model error.

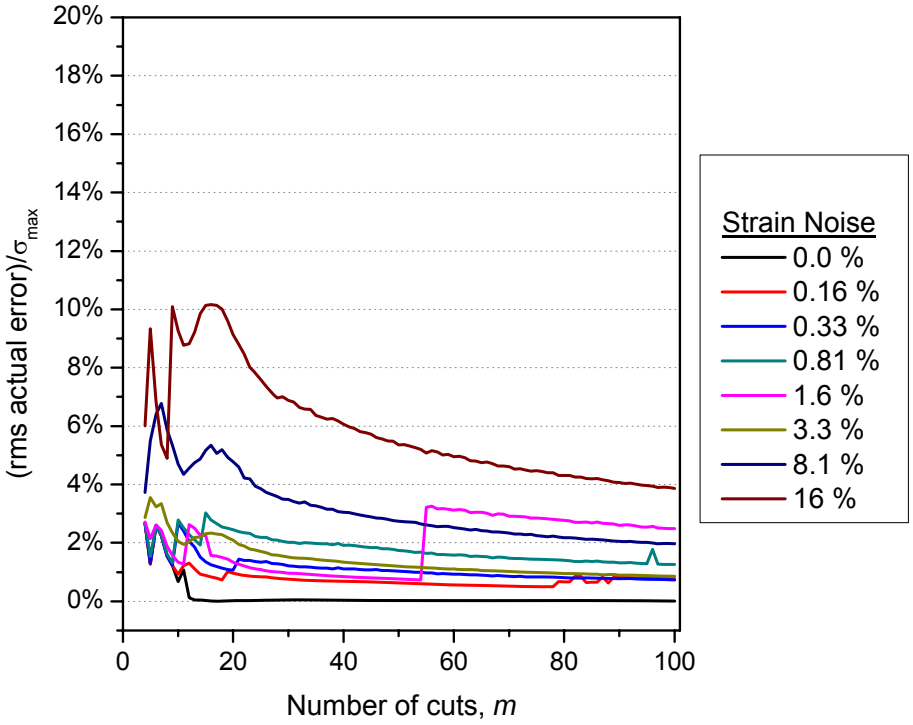


Figure 9. Estimated measurement uncertainty.

## Conclusions

A single stress profile, Figure 2, was considered in this study. Nonetheless, some general conclusions can be made.

- Even under extremely low noise/error conditions, 25 cuts should be considered the minimum both for achieving relatively low errors in the stress distribution and for an accurate uncertainty estimate.
- Under higher noise conditions, and probably also for more complicated stress profiles, more cuts result in better solutions. Considering the inability to estimate errors or the stress profile *a priori*, 40 or more cuts is probably a good idea.
- The selection of optimal order based on minimizing the estimated total uncertainty is generally effective. However, because of the stochastic nature of the problem, the true optimum is not always selected. It is suggested to supplement the procedure with careful examination of the fit to the strain data [1,4].
- The model uncertainty is key for an effective selection of the optimal expansion order and for a better estimate of uncertainty in the stress results.

## Acknowledgements

This work was performed at Los Alamos National Laboratory, operated by the University of California for the U. S. Department of Energy under contract number W-7405-ENG-36. Mr. Pagliaro's work was sponsored by a fellowship from the Universitá degli Studi di Palermo.

## References

[1] Prime, M. B., and Hill, M. R., 2006, "Uncertainty, Model Error, and Order Selection for Series-Expanded, Residual-Stress Inverse Solutions," Journal of Engineering Materials and Technology, **128**(2), pp. 175-185.
[2] Prime, M. B., 1999, "Residual Stress Measurement by Successive Extension of a Slot: The Crack Compliance Method " Applied Mechanics Reviews, **52**(2), pp. 75-96.
[3] Prime, M. B., and Hill, M. R., 2004, "Measurement of Fiber-Scale Residual Stress Variation in a Metal-Matrix Composite," Journal of Composite Materials, **38**(23), pp. 2079-2095.
[4] Hill, M. R., and Lin, W. Y., 2002, "Residual Stress Measurement in a Ceramic-Metallic Graded Material," Journal of Engineering Materials and Technology, **124**(2), pp. 185-191.